Heliyon 10 (2024) e24466

Contents lists available at ScienceDirect

Heliyon

journal homepage: www.cell.com/heliyon

Research article

Ecological spectroscopic methodologies for quantifying co-administered drugs in human plasma by photochemical quantum mechanical simulation

Maya S. Eissa [a], Khaled Attala [a,*], Ahmed Elsonbaty [a,**], Aziza E. Mostafa [b], Randa A. Abdel Salam [b], Ghada M. Hadad [b], Mohamed A. Abdelshakour [c]

[a] Department of Pharmaceutical Chemistry, Faculty of Pharmacy, Egyptian Russian University, Badr City, 11829, Egypt
[b] Department of Pharmaceutical Analytical Chemistry, Faculty of Pharmacy, Suez Canal University, 41522, Ismailia, Egypt
[c] Department of Pharmaceutical Analytical Chemistry, Faculty of Pharmacy, Sohag University, Sohag, 82524, Egypt

ARTICLE INFO

Keywords:
Greenness by design
Genetic algorithm
Molecular dynamics simulation
Photochemical quantum mechanical simulation
Fourier self-deconvolution
Agree greenness protocol

ABSTRACT

Urinary tract infections (UTIs) constitute the second most prevalent bacterial infections in the elderly demographic. The treatment landscape involves various antibiotics targeting the causative organisms; nevertheless, the emergence of resistance significantly impacts therapeutic effectiveness. Presently, a fixed-dose pharmaceutical combination is advocated to optimize patient outcomes by mitigating the risks of bacterial resistance and associated side effects. Ofloxacin (OFL) and cefpodoxime proxetil (CPD) combinations, co-administered with flavoxate hydrochloride (FLV), have demonstrated efficacy in UTI cases, offering relief from concomitant symptoms. In the pharmaceutical market, fixed-dose combinations have gained prominence, driven by advantages such as enhanced patient medication adherence and compliance. In the realm of analytical chemistry, the integration of green practices in the initial phases of method development is exemplified by the Greenness by Design (GbD) strategy. While univariate spectroscopic methods are conventionally considered suboptimal compared to chemometric techniques for resolving intricate mixtures, GbD approach, when applied to UV spectroscopy, enable univariate methods to attain comparable or superior outcomes. GbD adopts a systematic approach to optimize experimental conditions, minimizing environmental impact and maximizing analytical performance. Critical to GbD applications in UV spectroscopy is solvent selection, influencing spectral resolution and measurement sensitivity. GbD employs a combination of in-vitro and in-silico experiments to evaluate solute-solvent interactions with underlying photochemical quantum phenomena affecting the resulting spectral morphology, identifying an optimal compromise solvent with high resolution and minimal ecological impact. Consequently, it facilitates the efficient resolution of spectral overlapping and determination of complex mixtures in UV spectroscopy using univariate methods. Comparative analysis with chemometric techniques, acknowledged as potent spectral resolving methods, demonstrated that GbD-based univariate methods performed equivalently. The methodology was validated according to ICH recommendations, establishing a linear quantitation range (2–30 μg/mL) and a limit of detection (0.355–0.414 μg/mL) for the three drugs in human plasma. The greenness of the developed

* Corresponding author.
** Corresponding author.
E-mail addresses: Khaled-attala@eru.edu.eg (K. Attala), Ahmed-elsonbaty@eru.edu.eg (A. Elsonbaty).

https://doi.org/10.1016/j.heliyon.2024.e24466
Received 23 October 2023; Received in revised form 7 January 2024; Accepted 9 January 2024
Available online 16 January 2024

methodology was affirmed through the AGREE assessment protocol, confirming its environmentally conscious attributes.

1. Introduction

Urinary tract infections (UTI) are the second most common infections after otitis especially among the elder population and have a prevalence of about 14–16 % of bacterial infections. E. coli is the most common causative organism for the UTI. UTIs can be uncomplicated with mild symptoms as in cystitis or it can take the complicated form as in pyelonephritis and if untreated properly may precipitate chronic insults to the renal system [1]. Several types of antibiotics are used to eradicate the infection in UTI. Due to the nature of the potential bacteria causing UTI as most of them are gram negative organisms the most suitable classes of antibiotics would be fluoroquinolones, aminoglycosides, third generation cephalosporins and tetracyclines. Ofloxacin (OFL) and Cefpodoxime (CPD) are two examples of two different antibiotics (floroquinolone and cephalosporin, respectively) used in the treatment of UTI. OFL, a fluoroquinolone, exhibits its primary mode of action by impeding bacterial DNA gyrase. When tested in a laboratory setting, it demonstrates a wide range of efficacy against both aerobic Gram-negative and Gram-positive bacteria. However, its effectiveness against anaerobic bacteria is notably limited [2]. CPD belongs to the class of cephalosporin antibiotics. Its mechanism of action involves halting the proliferation of the bacterial cell wall. It exhibits a particular affinity towards penicillin binding protein 3, thereby impeding the synthesis of peptidoglycan, which serves as the principal constituent of bacterial cell walls. Consequently, this leads to an impairment in the construction of a fully functional cell wall, ultimately culminating in the demise of the bacterial cells due to osmotic lysis [3]. Both OFL and CPD are used separately or in combination as latest clinical studies revealed that the patient get benefits from the combined use of these two antibiotics to eradicate the causative organism and prevent the growth of resistant strains [4,5]. The development of fixed dose single tablets combining two or more drugs is an effective strategy towards enhancing the patient compliance and adherence to the medication and due to synergism in some instances the adverse effects are also lowered. As patients with UTI also suffer the accompanying lower urinary tract symptoms (LUTS) as urgency and pain, Flavoxate hydrochloride (FLV) is another suitable agent that is co-administered during UTI to control these symptoms [6]. FLV is an antispasmodic drug, acting by relaxing smooth muscles of the urinary tract so relieving the accompanied LUTS [7]. FLV achieves bladder relaxation by a combination of calcium antagonism and phosphodiesterase enzyme inhibition with minimal anticholinergic side effects noticed in other agents belonging to the same class [8]. By combining antibiotics with FLV the UTI patient will benefit from both infection eradication and symptoms relief during the course of the treatment.

Literature review revealed several spectroscopic [9,10] and chromatographic [11,12] methods for the determination of OFL in combination of either FLV or CPD binary mixtures. These methods were defective in determining the three drugs in their potential future fixed dose combinations or in plasma after concomitant administration.

The development of future fixed dose pharmaceutical combinations requires powerful and simple analytical methods that are cost effective [13–16]. In a previous study, we demonstrated the effectiveness of the greenness by design approach (GbD) in the swift development of eco-friendly analytical methodologies for resolving and determining complex pharmaceutical mixtures. In UV spectroscopy, GbD guides the analyst to optimize the solute-solvent interactions, which can reduce the peak broadening of the compounds' spectral bands. This optimization is important for resolving severely overlapping mixtures using simple mathematical methods, rather than using the multivariate methods that are longer and require more data to formulate their mathematical models [17].

To analyze the solute-solvent interactions, we use molecular dynamics simulations (MD) to calculate the non-bonding interaction and solvation energies which determine the magnitude of solute-solvent interactions [18]. We also use quantum mechanical (QM) analysis of the investigated compounds to reveal information about their excited states, the contributing molecular orbitals (MOs), the relation between the stability of each excited state and the utilized solvent, and the resulting morphology of the UV spectrum of each compound. The time dependent density functional theory (TD-DFT) simulations are the most suitable tool for the task of spectral analysis of the investigated compounds on the quantum level.

Unlike our previous study [19], which focused on the conceptualization of the GbD and its application in developing UV spectroscopic methods, the current study provides a deeper illustration of the photochemical quantum properties of each molecule in various solvents. It also extends the QM analysis of the solute-solvent interactions beyond the promising solvent identified after analyzing both the MD and full width at half maximum (FWHM) data. Moreover, it establishes the link between the hydrogen bonding (HB) with the solvent, the molecular spin multiplicity, and the gap energy (ΔE) of the excited state. This trinity is highlighted and demonstrated in the current study to address the limitations of the previous work.

The main objective of the current work is to develop univariate methods based on GbD concepts and multivariate approaches for the simultaneous analysis of OFL, FLV and CPD in their synthetic fixed dose combination and spiked human plasma. We also provide a thorough statistical comparison of the analytical performance of both approaches with the reported work.

2. Experimental

2.1. Reagents and materials

EPICO Pharmaceutical company generously provided Ofloxacin (OFL), Flavoxate hydrochloride (FLV), and cefpodoxime proxetil (CPD) with certified purity of 98.63 ± 0.43, 99.61 ± 0.51, and 99.74 ± 0.62. HPLC grade methanol and acetonitrile were supplied by

Sigma-Aldrich (Germany). Sodium bicarbonate was purchased from El Nasr Co, Egypt. Pharmaceutical formulation Genurin® Tablets (200 mg FLV) was obtained from the Egyptian pharmaceutical market, while Zipod O® Tablets (200 mg of each OFL and CPD) were bought online from a chain Indian pharmacy (Medplus, Mumbai, India).

2.2. Software and instrumentation

All spectrophotometric measurements were performed with a V-630 dual-beam UV–visible spectrophotometer (JASCO, Japan) and Spectra Manager V.2 software. Rotary evaporator (Scilogex-RE 100-pro, USA), Elma E30H ultrasonic device (Elmasonic, Germany) and K2015R Refrigerated Centrifuge (Centurion Scientific Ltd, UK) were utilized in dosage form and biological samples preparation.

All chemometric techniques were computed using MATLAB® R2015a (8.2.0.701) (The Math Works, Inc., Natick, Massachusetts, USA). The PLS and GA were carried out with the help of the PLS toolbox software version 2.1. MOE® 2015 was used to generate the 3D structures of the compounds under consideration, performing molecular dynamics simulations (MD) and calculating solvation and interaction energies. Avogadro® and Iboview® were utilized in preparing the input files for the TD-DFT calculations and to visualize the generated molecular orbitals. ORCA® 5.0.4 was utilized in running the TD-DFT calculations including excitation states, corresponding molecular orbitals and gap energies.

2.3. Evaluating the impact of solvent on solute spectral properties

The main objective of the current study is to settle the GbD concept in developing eco-friendly UV spectrophotometric methods capable of resolving complex mixtures with minimal analytical effort utilizing univariate mathematical methods. Additionally, this study tests the hypothesis that the solvent selection can influence the hydrogen bond (HB) interactions between the solute and solvent molecules and the band gap energy of the excited states which affect the degree of broadening of the resulting UV spectra and the consequent signal interference. Moreover, this study tends to provide illustrations of the involved electronic transitions abundance in each molecule under each different solvent and the relation between the electronic transition abundance with the spin multiplicity state of each molecule.

The phenomenon of solute-solvent interactions was investigated both in-silico and in-vitro modes. For in-vitro investigations; The effect of each solvent on the spectral morphology of the three compounds was investigated by preparing a stock solution of (200 μg/mL) in distilled water for each compound, then 10 μg/mL dilutions were prepared utilizing each solvent at a time as diluent. The full width at half maximum (FWHM) of the main peak on each spectrum was computed directly at two carefully selected wavelengths on the Lorentzian peaks. The FWHM tool was utilized as an in-vitro parameter to investigate the effect of each solvent on the spectral morphology regarding peak width.

The in-silico investigations aiming for choosing the most suitable solvent for the quantitation process was performed by engaging MD simulations with mechanical analytics conducted on the resulting trajectories augmented by spectral scanning of each component in each different solvent.

Furthermore, QM calculations were conducted to evaluate the effect of each tested solvent on the band gap energy (ΔE) of the excited states in each molecule with the elucidation of the predicted spectrum of each compound to confirm their identity.

2.3.1. Molecular dynamics simulations

MD simulations were conducted to in-silico investigate the effect of solute-solvent interactions on the molecular level. Structures of each compound were built in the MOE software depending on the smiles codes of each compound retrieved from the PubChem database. The structures were protonated at pH 7, potential charges were calculated and molecules were energetically relaxed regarding the Amber10: EHT forcefield parameters. The MD simulations were conducted in solvent environment utilizing water, methanol and acetonitrile and the Born implicit solvation model. The Nose-Poincare-Andersen (NPA) equations of motion were utilized to launch the simulation with sampling time of 0.5 Ps and a total simulation time of 760 Ps infiltrated by 30 Ps of heating period from 0 K to 300 K, 100 Ps equilibration period, 600 Ps production period and finally another 30 Ps cooling down period (300 K–0 K). By the end of the simulation time; trajectories were generated and utilized in mechanical analytics calculations as solvent-solute interaction energies and solvation energies.

2.3.2. TD-DFT and molecular orbitals calculations

The B3LYP hybrid functional was utilized as the main functional during the conducted TD-DFT calculations with the RIJCOX functional and the split valence polarization function (def2-SVP). The solvent model CPCM was utilized for the three water, methanol and acetonitrile systems. By the end of the convergence the obtained data were analyzed regarding the calculated MOs, transition energies in each excited state and the predicted UV spectra of each compound in each different solvent.

2.4. Procedures

2.4.1. Standard solutions

Standard solution of each drug OFL, FLV and CPD were prepared by accurately weighing 20 mg of each standard and being transferred accurately to three separate 100 mL volumetric flasks and 80 mL of distilled water was added and the volumetric flasks were subjected to vigorous shaking and sonication in temperature controlled ice bath for 30 min eventually; the volume in the three flasks was completed by distilled water to obtain a standard of 200 μg/mL of each. The standard solutions were stored in dark and

refrigerated (4 °C) till use.

2.4.2. Construction of calibration curves

Several dilutions in the range of (2–40 μg/mL) for each were prepared by withdrawing suitable aliquots from each standard aqueous solution, transferred to three separate 10 mL series of volumetric flasks and volume was completed by methanol (HPLC grade) as diluent. The prepared dilutions of each standard (OFL, FLV and CPD) were scanned under UV spectrophotometer in the range of 200–400 nm against methanol as blank and the resulting spectra of each standard were recorded. The regression equation for each standard was then formulated according to each specified spectrophotometric method discussed below.

2.4.3. PLS and GA-PLS methodologies

A 5-level, 3-factorial design with five concentration levels (standards) for each of the three investigated components was used to construct 25 mixes. The mixed space is expanded by the used designs very well. The linearity and absorptivity of the mixtures were taken into account while selecting the concentration ranges. The used design's central level is 6 μg/mL OFL, 14 μg/mL FLV, and 14 μg/mL CPD. From a total of 25 combinations, 10 mixtures of the three developed medicines were selected for validation calculations, and the remaining 15 mixtures were used as calibration data **Table (1)**.

Table 1
The concentrations of the calibration and validation sets as calculated *via* implementing a 5-level, 3-factor experimental design approach (The shaded rows represent the validation set).

Sr.No.	OFL (μg/mL)	FLV (μg/mL)	CPD (μg/mL)
1	6	14	14
2	6	6	6
3	2	6	22
4	2	22	10
5	10	10	22
6	4	22	14
7	10	14	10
8	6	10	10
9	4	10	18
10	4	18	22
11	8	22	18
12	10	18	14
13	8	14	22
14	6	22	22
15	10	22	6
16	10	6	18
17	2	18	6
18	8	6	14
19	2	14	18
20	6	18	18
21	8	18	10
22	8	10	6
23	4	6	10
24	2	10	14
25	4	14	6

2.4.4. Fourier self-deconvolution method (FSD)

In this method the zero order spectra of OFL, FLV and CPD were deconvoluted at an FWHM of 40 to generate amplitudes which were then investigated for zero-crossing and no contribution areas to resolve their signals. At 339 nm the method could determine OFL in the presence of both FLV and CPD. A calibration curve for OFL at 339 nm in the concentration range of (2–14 μg/mL) was constructed and the regression equation was computed to determine OFL in the presence of both FLV and CPD with no interference from both in prepared lab mixtures, pharmaceutical dosage forms, and biological fluid. In the same context; the zero-order spectra were also deconvoluted at FWHM of 90 to generate amplitudes for the three components in which we could determine FLV at 325 nm in the presence of both OFL and CPD. At 325 nm a calibration curve for FLV in the concentration range of (2.5–30 μg/mL) was constructed and the regression equation was then computed to determine FLV in the prepared lab mixtures, biological fluid and pharmaceutical dosage form in the presence of OFL and CPD.

2.4.5. Dual wavelength spectrophotometric method (DW)

This method was developed for the determination of CPD in the presence of both OFL and FLV. The zero-order spectra of CPD, OFL and FLV were overlain and suspected for two wavelength points that their subtraction leads to cancellation of the OFL and FLV signal with a significant difference in the CPD absorbance that was correlated with the CPD concentration increment. These two wavelength points were 264 and 267 nm at which the difference in the OFL and FLV is approximately zero and the difference is corresponding to the increased concentrations of CPD. A calibration curve was constructed utilizing the difference in absorbance vs. CPD concentrations in the range of (6–30 μg/mL) and the regression equation was formulated for the determination of CPD in the presence of both OFL and FLV in prepared lab mixtures, biological fluid and pharmaceutical dosage form.

2.4.6. Analysis of the laboratory prepared mixtures

Several synthetic mixtures of OFL, FLV and CPD were prepared in varying ratios by accurately withdrawing suitable aliquots into a series of 10 mL volumetric flasks and volume was adjusted by methanol as a diluent. Each prepared lab mixture was scanned vs. methanol as a blank at wavelength range of (200–400 nm), then by applying the above methods and each corresponding regression equation the constituents of each lab mix was determined.

2.4.7. Application to pharmaceutical dosage form

The need for combined dosage forms that aid in patient adherence and compliance is a never end quest. The dosage form containing OFL and CPD already exists in the international market for the treatment of several bacterial infections as urinary tract infections (UTI), typhoid fever and bacterial prostatitis. During the course of a UTI infection the patient requires other medications relieving the symptoms as FLV which was proved as effective to decrease the pain and frequent urination during and after the recovery from UTI [20]. There is a potential window in the market for the development of a single dose combination comprising OFL, CPD and FLV for the purposes of eradication of bacterial UTI and the relief of the accompanying symptoms. To prepare such combined dosage form in lab we used already existing dosage forms to synthesis a mixed dosage form. A twenty tablet of genurine® (200 mg FLV) were weighed and the average weight was calculated, then were crushed into fine powder and homogenized. Another 20 tablets of Zipod O (200 mg of each OFL and CPD) were weighed and the average weight was calculated, then the tablets were treated as above. An equivalent weight of 2000 mg of FLV and 2000 mg of both OFL and CPD were accurately weighed from each corresponding powdered tablets to form a mixture. The weighed aliquots were mixed thoroughly and then another equivalent weight of 200 mg of OFL, FLV, and CPD were weighed accurately from the above mixture and transferred to a 200 mL volumetric flask containing 100 mL of distilled water. The flask was shaken vigorously for 3 min then was subjected to heat controlled sonication for 30 min finally the volume was adjusted with distilled water and a suitable volume was cool centrifuged (4 °C) at 10000 rpm for 10 min. A 5 mL aliquot was withdrawn from the clear supernatant and accurately transferred to another 50 mL volumetric flask. Finally, a 1 mL aliquot was transferred to a 10 mL volumetric flask and volume was completed with methanol to obtain a concentration of 10 μg/mL of OFL, FLV and CPD. A suitable volume was transferred to a quartz cuvette for UV spectroscopic scanning vs methanol as a blank, the resulting spectrum was recorded and manipulated as discussed above utilizing the corresponding regression equations to determine the concentration of each component.

2.4.8. Application to biological sample

A 1 mL of drug free plasma was transferred to a 15 mL falcon tube, mixed with 2 mL of 5 % sodium bicarbonate and spiked with 3 mL of methanolic solution composed of 3 μg/mL, 3 μg/mL and 15 μg/mL of OFL, FLV and CPD, respectively [21–23]. After mixing we added 5 mL of diethyl ether and the sample was vortexed for 5 min The ether layer was left to stand out, then the upper ether layer was decanted and subjected to cool centrifugation at 10000 rpm for 5 min The resulting supernatant was evaporated till dryness by rotary evaporator at 40 °C and was reconstituted into 3 mL methanol and the concentration of each component was determined by the corresponding spectrophotometric method as described before.

3. Results and discussion

In the last decade several developed analytical methods were nominated green based on an assessment implemented in the late phase of the method development. The strategy of utilizing the GbD approach involves employing both in-silico and in-vitro experiments to aid in the selection of the most suitable solvent that attains the necessary spectral resolution. This subsequently leads to a decrease in the analytical work and solvent disposal, ultimately resulting in more environmentally friendly outcomes as reflected by

the greenness assessment scales. Thanks to the GbD; greenness could be integrated within the early phases of the method development. In the realm of UV spectrophotometric methods development, the guiding principle of GbD centers around the meticulous selection of solvents. This selection process is based on a criterion that encompasses various factors including the FWHM of the principal peak, the interactions between solute and solvent, the energies associated with solvation, as well as the influence of the solvent on the transition states of individual molecules. The efficacy of this approach has been validated through its ability to successfully untangle intricate mixtures characterized by overlapping components, utilizing univariate spectroscopic methodologies. The multivariate chemometric methods represent the utmost spectral resolving method utilized to resolve such complex mixtures. GbD represents a window for the use of univariate methods in resolving these complex mixtures. The advantage of the univariate methods lays in being inherently simple as it requires no sophisticated software to implement spectral data and being time and effort saver.

The current study extends our previous work [19] on the conceptualization of the GbD approach for UV spectrophotometric methods development. Through the current work, we illustrated the photochemical quantum phenomena that affect the UV peak broadening and the degree of interference of different compounds in different solvents besides demonstrating how GbD can optimize the solvation effect to control the peak broadening of the UV spectrum of each compound from the photochemical quantum perspective. This enables the resolution of complex overlapping mixtures using simple univariate methods such as FSD and DW. Here in, we developed partial least square method utilizing the genetic algorithm (PLS-GA) besides the GbD guided univariate spectroscopic methods and compared their resolution efficiency with the reported methods.

3.1. Optimization of the solute-solvent interactions

Building on our previous work [19] we concluded that the type of the utilized solvent directly affects the morphology of the resulting UV spectrum of the scanned compound. Several factors play roles in this phenomenon as hydrogen bonding (HB) between the solvent and the solute molecules, the polarity of the solvent and its effect on the excitation states of the compound and spin multiplicity of the solute molecule itself.

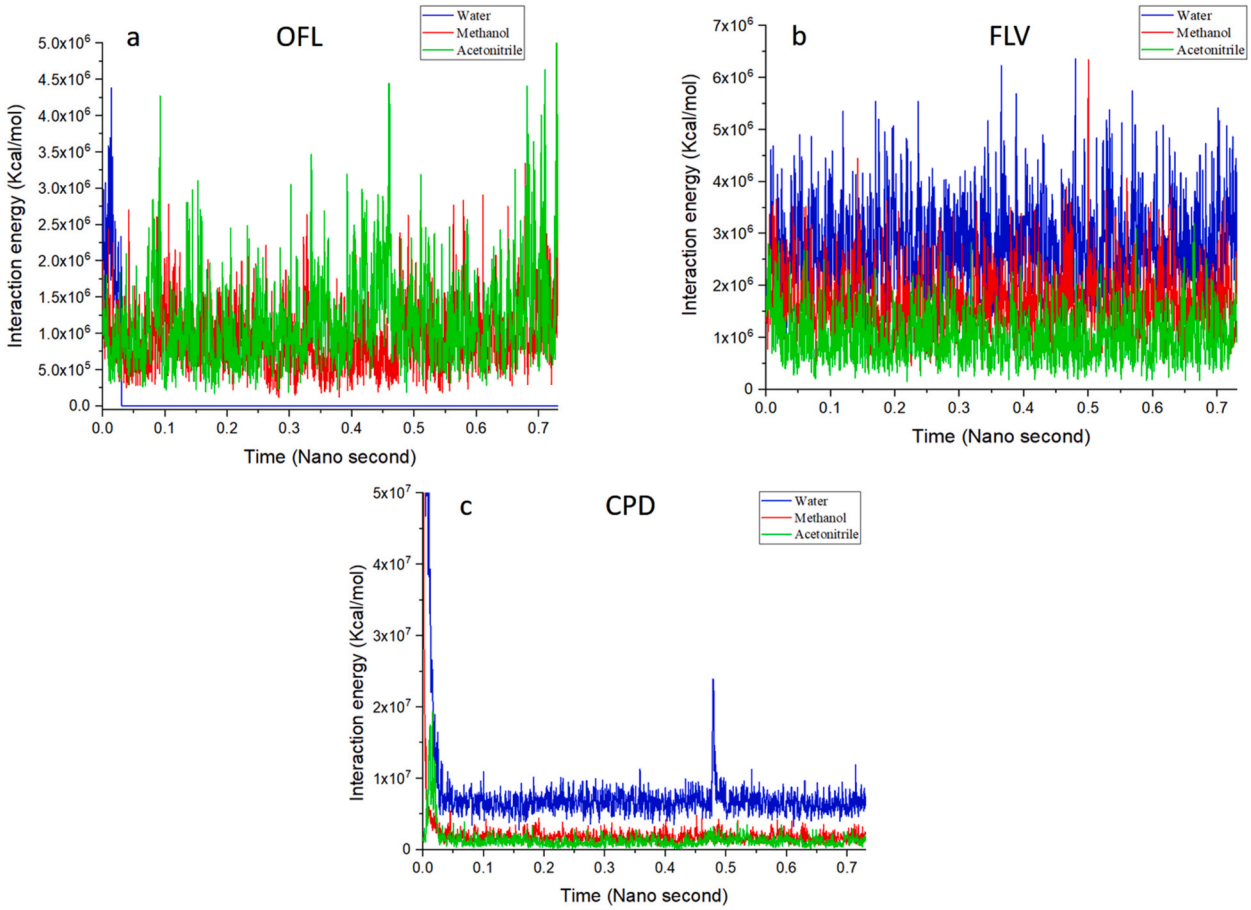

Fig. 1. a: Solute solvent interaction energy profile for the OFL in the three investigated solvents
Fig. 1 b: Solute solvent interaction energy profile for the FLV in the three investigated solvents
Fig. 1 c: Solute solvent interaction energy profile for the CPD in the three investigated solvents.

HBs when occur in one solvent they cause the spectrum of the compound to be more broad than in other solvents. This broadening contributes to the potential interferences with other spectra of the other compounds present in the same pharmaceutical mixture [24]. Peak broadening in UV spectrum of a compound due to HB with polar solvent molecules can be explained by the fact that HB stabilizes one excitation transition than another for example if a compound has a mixed excited state composed of both pi-pi* and n-pi* transitions occurring simultaneously, the HB affects the n-pi* transitions more by interacting with the non-bonding (HOMO) orbital so altering the molecular dipole moment [25]. The excitation of electrons to higher energy levels within a molecule leads to the creation of a charge separation and a dipole moment [26]. This dipole moment is influenced by the polarity of the surrounding solvent, which in turn impacts the stability of the excited state. In a polar solvent, the typically unstable n-pi* excited state becomes more stable and experiences a shift towards lower wavelengths. However, the polarity of the solvent also results in a broadening of the peaks in the spectrum of the compound. This is due to the varying distances and directions of interactions between the solute and the solvent. Each interaction causes a change in the dipole moment of the molecule, leading to distinct energy values for the same excited state (n-pi*). The broadening effect observed in the spectrum is a reflection of this variation [27].

The compound's spin multiplicity, which characterizes the potential spin states of a molecule based on its spin angular momentum (S), is also impacted by the polarity of the solvent. Polar solvents have a tendency to stabilize the ionized states of a compound, resulting in a modification of the equilibrium between its spin states. This modification can be observed in the compound's spectrum. For instance, OFL exhibits a spin state of triplet, whereas both CPD and FLV exhibit singlet states. The spectrum of OFL in different solvents would display varying characteristics, particularly in the FWHM of the primary peak(s). Furthermore, the TD-DFT analysis of the molecular orbitals of OFL, CPD, and FLV in both the ground and excited states revealed that these three molecules can undergo n-pi* and pi-pi* transitions. The choice of solvent would impact the UV spectrum of these molecules by altering the equilibrium between these transitions to varying degrees, depending on the interactions with the solvent as seen in Fig. S1 (a-c).

3.1.1. *Analysis of MD simulations to optimize solute-solvent interactions*

The examination of the MD simulations trajectories (Figure S2 (a-c)) allows for the investigation of the interactions between solute and solvent. It was observed that water, being the most polar solvent, exhibited the highest frequencies of solvent interactions. These interactions were primarily due to HB and dipole interactions in the cases of FLV and CPD (Fig. 1(a–c)). Additionally, the calculation of solvation energies indicated an exothermic dissolution pattern in water for both CPD and FLV, suggesting strong interactions between their solute and water molecules. These findings were consistent with the calculated interaction energies in each scenario. In the case of OFL, acetonitrile displayed the highest interaction energies, primarily driven by HB and dipole-dipole interactions (Fig. 1 (a)). This was also reflected in the solvation energies (Figure S3 (a-c)). Based on these preliminary indications of solute-solvent interactions, water was excluded as a solvent due to its extensive HB and dipole interactions, which were predicted to have a negative impact on the

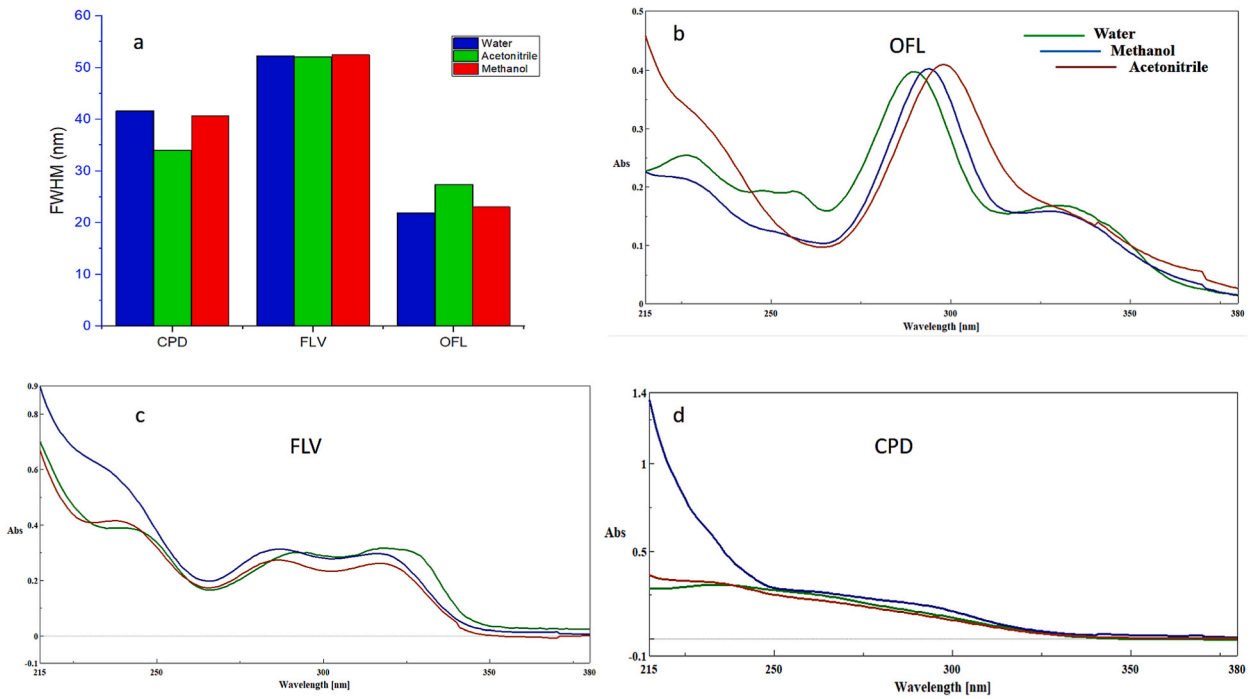

Fig. 2. a: The experimentally determined full width at half maximum (FWHM) for the three drugs based on each drug major peak in the three investigated potential solvents. Fig. 2 b: The experimentally scanned overlaid spectra for OFL in the three potential candidate solvents. Fig. 2 c: The experimentally scanned overlaid spectra for FLV in the three potential candidate solvents
Fig. 2 d: The experimentally scanned overlaid spectra for CPD in the three potential candidate solvents.

resulting spectra in the cases of CPD and FLV. Furthermore, the FWHM of the major peaks on each compound spectrum was determined using the Lorentzian equation, which agreed with the analysis of the interaction energies data (Fig. 2 (a)). The FWHM of CPD and FLV in water exhibited broadening in their major peaks, while in the case of OFL, acetonitrile was the solvent responsible for the broadening effect. The peculiar behavior of OFL can be explained by its unique status as the only compound in the triplet state, resulting in a more complex equilibrium between its spin states. As observed experimentally, acetonitrile, rather than water, caused an imbalance in this equilibrium by preferentially stabilizing one of the spin states of OFL over the others, leading to the observed effect. The fluctuations in FWHM of FLV in the three solvents were relatively insignificant. Therefore, by focusing the comparison between OFL and CPD, it can be concluded that acetonitrile was excluded as a solvent due to the severe broadening effect it had on OFL [28].

So, after this thorough analysis of the given data from interaction, solvation energies, FWHM and the molecular orbitals we could initially recommend methanol as a compromise solvent for the analysis process for its lowered effects on the broadening of the three compounds spectra which also decreased the overlapping in their lab mixtures to resolve these compounds utilizing both univariate and multivariate spectrophotometric methods.

3.1.2. TD-DFT simulations and molecular orbitals calculations

The TD-DFT studies provided a theoretical explanation for the observed effects of the solvent on the UV spectra of the investigated compounds, which was relevant and necessary for our research. The TD-DFT analysis revealed how the electronic transitions and their gap energy, which are related to the potential peak broadening, varied with different solvents. The peak broadening was the response that we wanted to optimize for the solvent factor addressed by GbD. Thus, the TD-DFT studies complemented the experimental results and helped us to understand the underlying quantum photochemical mechanisms of the solvent effects on the UV spectra of the investigated compounds.

The performed TD-DFT simulations for the three investigated compounds was implemented in solvated environment utilizing the CPCM solvation model using the key words water, methanol and acetonitrile to investigate the effect of each solvent on each molecular electronic structure and excited states. After the completion of the convergence of each simulation the excited states data were treated to calculate the spatial orientation of MOs involved in each excited state.

By investigating these MOs for each compound we found that the electronic excitations were composed of complex n-Pi* and Pi-Pi* transitions as seen in Figure S1 (a-c). This observation served as the primary source of disparities in the morphology of the experimentally derived UV spectra for each compound in various solvents, as depicted in Fig. 2 (b-d). The rationale behind this lies in the fact that each solvent displayed a distinct stabilizing influence on the equilibrating transitions, thereby impacting the peak positions and intensities. For instance, water exerted a potent stabilizing effect on the transitions of CPD and FLV, while acetonitrile displayed a robust stabilizing effect on the transitions of OFL. These effects were intricately associated with the interactions between the solute and solvent, as discussed in the previous section.

The predicted UV spectra of each compound were plotted utilizing the output data of the TD-DFT calculations in methanol Fig. S4 vs. the experimentally obtained spectra and as noticed there was agreement between both spectra indicating accuracy of the conducted calculations in solvated environment.

The gap energy (ΔE), representing the energy difference between the HOMO and LUMO orbitals, was calculated for each compound in each solvent and was represented graphically to compare the effect of each solvent on the transition energy required for excitation Fig. S5. It is known that the n-Pi* transitions are always lower in transition energy than the Pi-Pi* transitions in other words the ΔE of

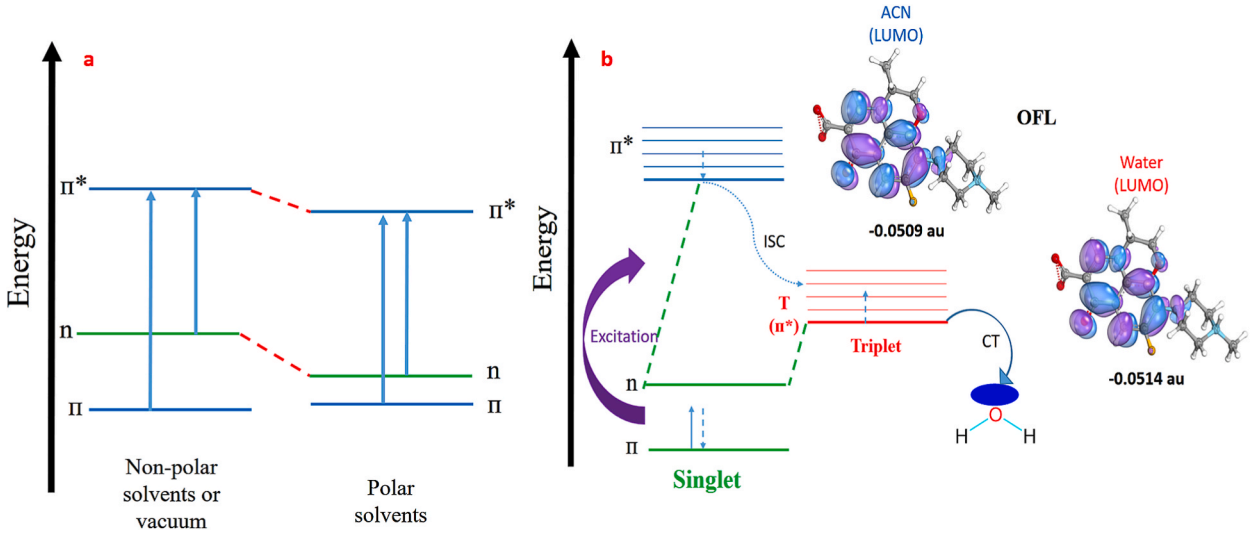

Fig. 3. a: The solvatochromic effect of different environments on the transition energies of both pi-pi* and n-pi* electronic transitions Fig. 3 b: Illustrating the probability of intersystem crossing (ISC) process occurring in OFL showing the charge transfer (CT) complex formation with water and the accompanied energies of LUMOs for OFL in water and acetonitrile solvents.

the n-pi* transitions is lower than that of the pi-pi* transitions. This concept is only correct in the non-polar environment or in vacuum. However, the incorporation of a polar solvent may change this situation by what is known as solvatochromism [29]. The polar solvent has un equal effects on both the n (non-bonding) and the pi* anti-bonding orbitals. The polar solvent always tends to interact more *via* HB interactions with the lone pair electrons in the n orbitals than the excited electrons in the pi* orbitals resulting in more significant stabilization of the n (HOMO) than pi* (LUMO) orbitals so decreasing the energy of the n orbitals in a way that increases the ΔE of the n-pi* transitions as illustrated in Fig. 3 (a) [30].

The data presented on Fig. S5 complements the conclusions made from Fig. 2 (a); as water is the most polar solvent it tends to interact with the n orbitals in the compounds FLV and CPD leading to more stabilization of their HOMO (n) orbitals leading to elevation in the ΔE which is also an indication for potential broadening and depressed intensity in their spectrum as confirmed by their corresponding FWHM values and in-vitro determined spectra as shown earlier.

Acetonitrile is less polar than water and has a lower capability of establishing HB with the non-bonding HOMO orbitals in both FLV and CPD. Therefore, the values of ΔE in case of acetonitrile were significantly lower than those of water and methanol, confirming the probability of more abundant pi-pi* transitions in acetonitrile. This is because acetonitrile can interact and stabilize the pi* orbital by dipole-dipole interactions, explaining the depressed ΔE values. Methanol has a moderate potential of establishing HB with the HOMO (n) orbitals of both FLV and CPD, as revealed by their elevated interaction energies with methanol in Fig. 1 (b&c). At the same time, methanol causes a slight increase in the ΔE values in both compounds compared to acetonitrile.

OFL, as mentioned earlier, is the only compound with a different spin multiplicity tending to achieve the triplet state upon excitation which is the reason for its odd behavior in the same solvent in both FWHM and band gap energy plots [28]. OFL has a pyridobenzoxazine ring and fluorine atom, which both provide a highly conjugated system and heavy atom effect, enabling the orbitals overlapping, acting as donors or acceptors for charge transfer (CT) complexes, and potentiating the probability of intersystem crossing (ISC) [31]. OFL seems to undergoes ICS upon excitation to an antibonding orbital of lower energy establishing a charge transfer complex with water molecules (acting as the acceptor) leading to exceptional lowering in the ΔE of OFL in water, rather than as expected and seen in the FLV and CPD (Fig. 3 (b)).

Acetonitrile could have been considered as the solvent of choice in case of FLV and CPD, but it was not suitable due to the depression in signal intensities in FLV and CPD, affecting the sensitivity of the developed method and the odd behavior of this solvent in case of OFL. One can exclude water here due to the extensive HB and the resulting broadening caused in FLV and CPD, making their resolution from OFL a challenging task. Both acetonitrile and methanol in case of FLV showed no significant difference regarding the

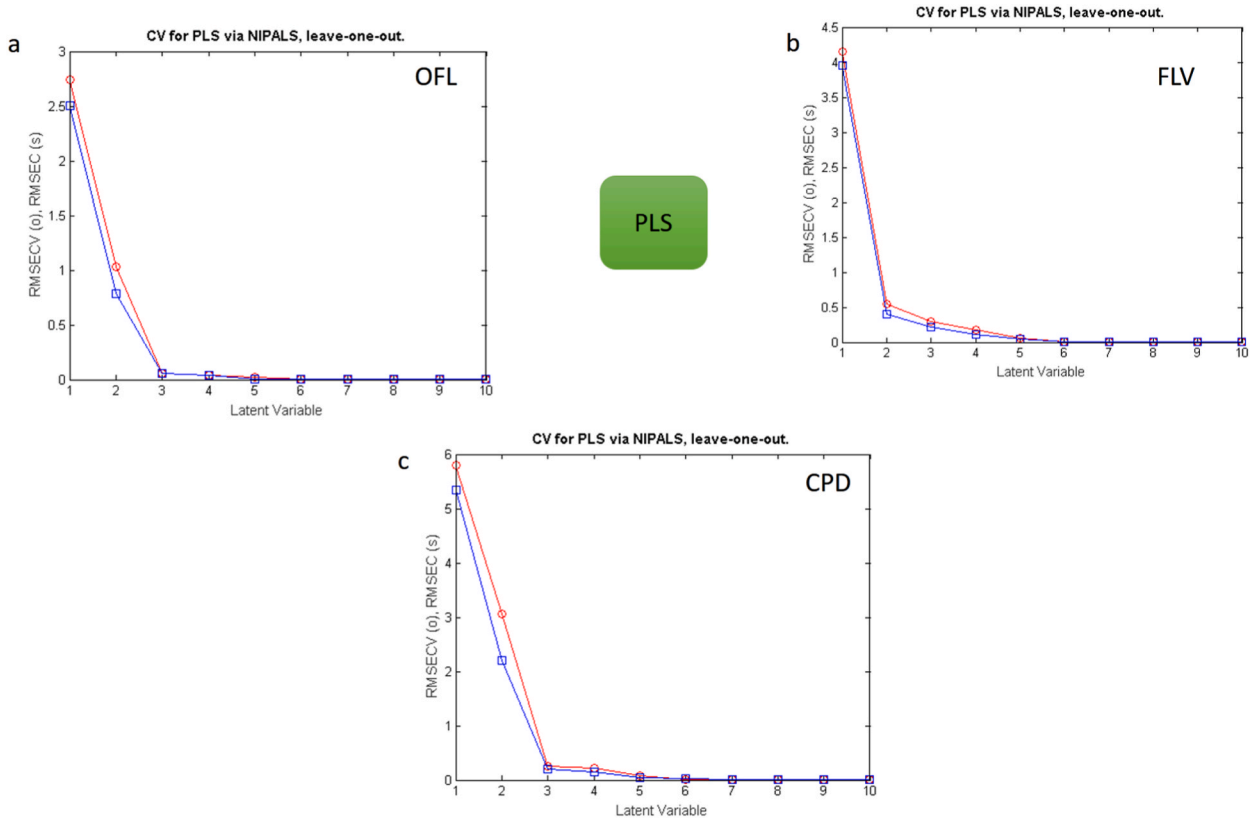

Fig. 4. a: Latent variables plot for the PLS based model for the determination of OFL. Fig. 4 b: Latent variables plot for the PLS based model for the determination of FLV. Fig. 4 c: Latent variables plot for the PLS based model for the determination of CPD.

ΔE and FWHM values, so FLV can be set aside. The CPD and OFL when compared regarding the ΔE and FWHM values. We can conclude that methanol is the most suitable as a compromise solvent. Besides, the resolution of OFL from CPD represented a challenge during the early trials of method development. Which necessitated the objectivity of reducing the potential peak broadening in these two compounds.

3.2. Application of the developed UV spectroscopic methods

3.2.1. PLS and GA-PLS methods

In this Investigation, the absorbance matrix of the calibration dataset was stratified using the partial least squares (PLS) regression approach, which is widely used to project data into new conceptual spaces. The prior knowledge of the concentration values associated with each standard specimen served as the basis for this transformation. The foundation for dimensionality in this newly created space was provided by the latent variables, which are characterized as linear combinations of the initial predictor variables. Notably, choosing the right number of latent variables was a vital parameter that required careful calibration to prevent over fitting in the final model. A cross-validation strategy was used to determine this ideal count. One analyte was sequentially eliminated from the calibration spectra at a time, and PLS was then used to model the spectra without the excluded analyte. The Root Mean Square Error of Cross-Validation (RMSECV) was then calculated by gradually adding more latent variables to the model. Adhering to the criterion set by the Haaland and Thomas criteria [32], the optimal number of latent variables was determined to be the number at which the model using the most latent variables showed no statistically significant difference in Cross-Validated Prediction Error Sum of Squares (PRESS) when compared to the model using the fewest latent variables.

The chance of each additional component significantly contributing to the model reduced as the marginal differences between the lowest Root Mean Square Error of Cross-Validation (RMSECV) and other RMSECV values grew smaller. Notably, our research showed that for OFL and CPD, three latent variables best explained the regression model, whereas for FLV, four latent factors worked best, as shown graphically in Fig. 4 (a-c). We calculated and presented a number of validation metrics, including the Root Mean Square Error of Calibration (RMSEC), Root Mean Square Error of Prediction (RMSEP), Relative Root Mean Square Error of Prediction (RRMSEP), and the Bias-Corrected Mean Square Error of Prediction (BCMSEP), **Table (2)**, to evaluate the model's effectiveness and its ability to predict.

We used the Genetic Algorithm (GA), a method of variable selection, to eliminate uninformative variables in order to improve the performance of the Partial Least Squares (PLS) model. This method was used to reduce redundancy and keep useful variables in a dataset with 120 variables that ranged in wavelength from 210 to 330 nm. As shown in **Table (3)**, many factors impacting the GA operation were adjusted. Population size was discovered to have a substantial effect on GA performance among these variables. Smaller populations have limited capacity to explore the solution space, which resulted in less-than-ideal outcomes, whereas larger numbers enabled more thorough solution search but ran the risk of premature convergence. The proportional link between population size and convergence rate was highlighted by this.

The cross-over rate was another crucial variable that was crucial in moldings the genetic population and guiding it in the direction

Table 2
Validation results of OFL, FLV, and CPD by the proposed chemometric methods.

Drug	RMSEC		RMSEP		RRMSEP		BCMSEP		RMSECV	
	Model									
	PLS	GA-PLS	PLS	GA-PLS	PLS	GA-PLS	PLS	GA-PLS	PLS	GA-PLS
OFL	0.05850	0.02496	0.05129	0.02377	0.94995	0.44010	0.00263	0.00056	0.0543	0.01290
FLV	0.11671	0.07502	0.1615	0.10209	1.26168	1.70115	0.02608	0.01042	0.1720	0.00150
CPD	0.19880	0.08383	0.25177	0.11169	0.79757	0.75467	0.06339	0.00124	0.2604	0.13260

Table 3
The optimized parameters of genetic algorithm selected as variable selection procedure to enhance the PLS models predictability.

Parameters	Optimum values		
	OFL	FLV	CPD
Population size		36	
Maximum generations		100	
Mutation rate		0.005	
Wavelength used at initiation		15	
The number of variables in a window (window width)		1	
Percent of population (% of convergence)		90	
Cross type		Double	
Maximum number of latent variables	3	4	3
Cross validation		Random	
Number of subsets to divide data into for cross validation		15	
Number of iterations for cross validation at each generation		3	

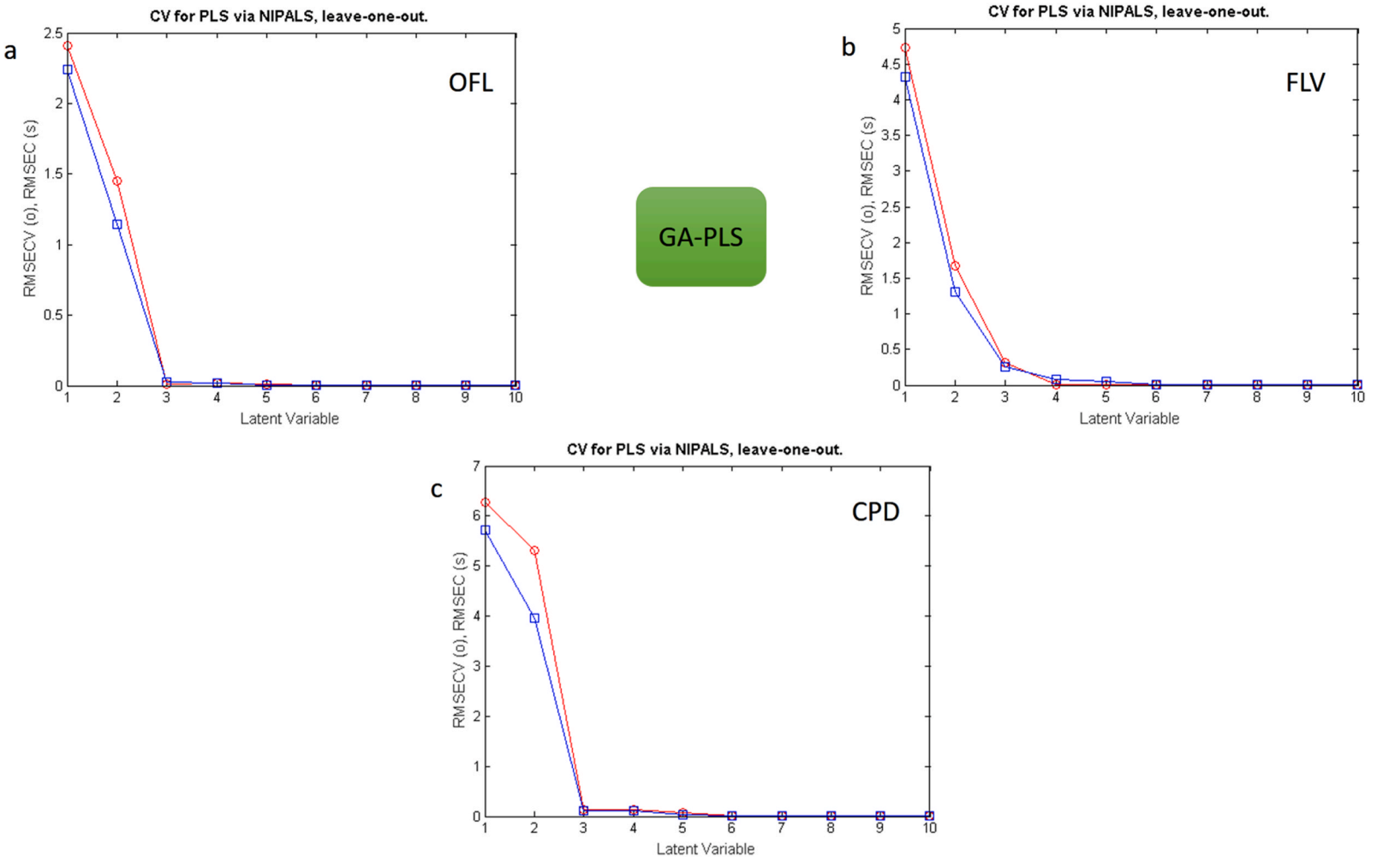

Fig. 5. a: Latent variables plot for the GA-PLS based model for the determination of OFL. Fig. 5 b: Latent variables plot for the GA-PLS based model for the determination of FLV Fig. 5 c: Latent variables plot for the GA-PLS based model for the determination of CPD.

of universally ideal solutions. Lower rates prevented the introduction of innovative solutions, limiting population variety and exploration, whereas higher cross-over rates permitted rapid adaption to new solutions. Additionally, by changing one or more chromosomal genes, the mutation rate which is used to preserve genetic variety within the population is carefully regulated to prevent early convergence.

The number of subsets, the maximum number of latent variables, and the number of iterations were also examined as additional GA factors. By using GA, we were able to successfully reduce the absorbance matrix's variable count between 13 and 23 % of the original matrix, resulting in inputs with fewer variables (particularly, 28, 16, and 21 variables for OFL, FLV, and CPD, respectively). Importantly, this decrease in complexity resulted in better model recoveries without compromising the preservation of the same latent variables as in the original PLS model as seen in Fig. 5 (a-c). The validation findings shown in **Table (2)** confirmed these changes, demonstrating the success of our method in creating simpler and more useful models.

3.2.2. FSD and DW spectrophotometric methods

Thanks to the application of GbD which guided us through optimizing solute-solvent effect to limit the resulting spectral band broadening and reducing the potential overlapping in the investigated ternary mixture; simple mathematically based spectrophotometric methods as FSD and DW could be applied to resolve the components of the mixture so reducing the exerted analytical effort to quantify complex mixtures.

The FSD method was developed to resolve and determine both OFL and FLV simultaneously and in the presence of CPD. This method is a simple mathematical method acting by deconvoluting the original spectra so that their band widths are reduced to an extent that permits the resolution of the complex spectral mixture. By controlling the deconvolution factor (FWHM, being 40 for OFL and 90 for FLV) the deconvolution algorithm uses the intrinsic line-shape of the original signal as a filter during the process resulting in narrow bands infiltrated by zero-crossing or no contribution spots which are utilized in resolving the overlapping signals of the ternary lab mixture Fig. 6 (a-b). The corresponding regression equations were computed after calibrating the amplitudes values of OFL signal at 339 nm in a range of (2–14 μg/mL) and those of FLV at 325 nm in a range of (2.5–30 μg/mL) as summarized in **Table (4)**.

In DW, two wavelength points were carefully selected so that by applying subtraction the signals of the interfering components (OFL and FLV) were eliminated and a difference in the CPD signal (ΔP 264 &267 nm) is correlated to its concentration in a range of (6–30 μg/mL) as in Fig. 6 (c) and data were summarized in **Table (4)**.

The OFL, FLV and CPD concentrations in their ternary lab mixtures **Table (5)** and pharmaceutical dosage form **Table (6)** were determined utilizing each corresponding regression equation.

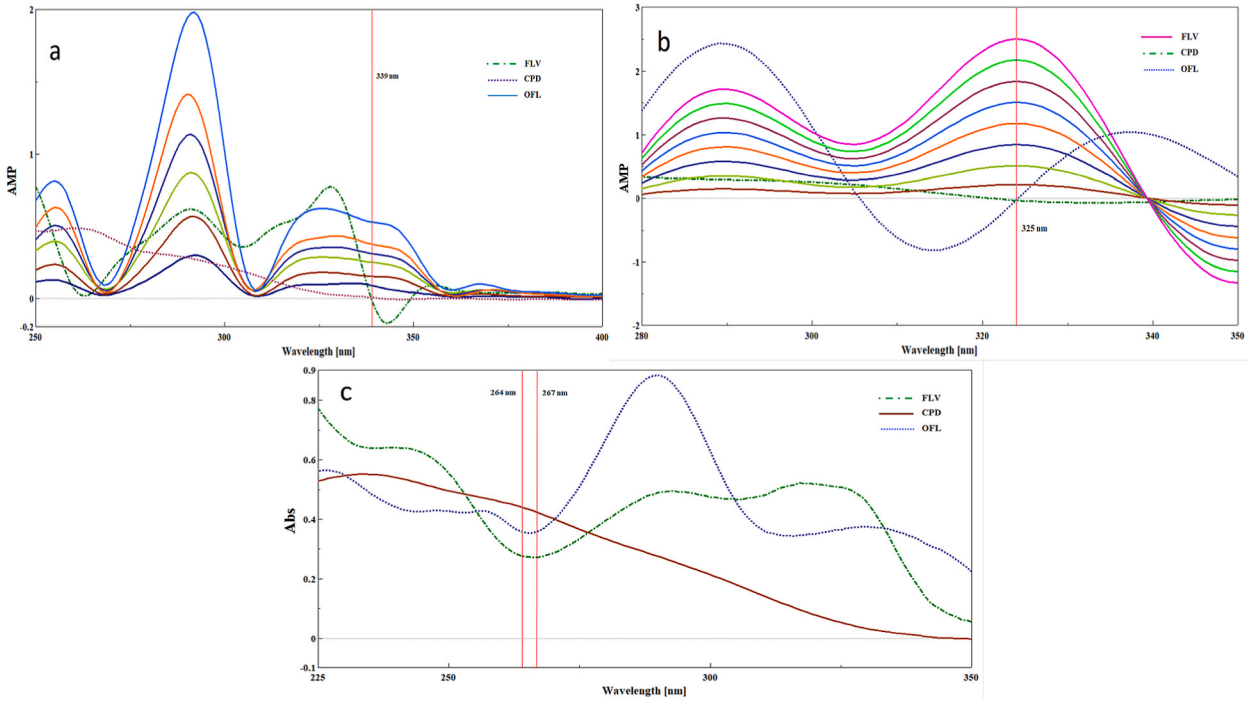

Fig. 6. a: Calibration for the FSD based spectrophotometric method for the determination of OFL in the range of (2–14 μg/mL) in the presence of both CPD and FLV. Fig. 6 b: Calibration for the FSD based spectrophotometric method for the determination of FLV in the range of (2.5–30 μg/mL) in the presence of both CPD and OFL

Fig. 6 c: Calibration for the DW based spectrophotometric method at 264 and 267 nm for the determination of CPD in the range of (6–30 μg/mL) in the presence of both OFL and FLV.

Table 4
Summary of Calibration data for the analysis of OFL, FLV, and CPD.

Validation parameters	OFL	FLV	CPD
	FSD	FSD	DW
Wavelength (nm)	339	325	264&267
Linear range (μg/mL)	2–14	2.5–30	6–30
Slope	0.0313	0.0819	0.0009
Intercept	0.0454	0.0228	0.0001
Correlation Coefficient (r)	0.9996	0.9998	0.9998
LOD (μg/mL)	0.355	0.457	0.414
LOQ (μg/mL)	1.075	1.384	1.254
Accuracy (Recovery % ± SD)[a]	99.95	99.94	101.16
	±0.594	±0.292	±0.495
Precision (RSD) Intra-day[b]	±0.653	±0.254	±0.546
Inter-day[c]	±0.668	±0.344	±0.555

[a] Mean of five determinations.
[b] Mean of three various concentrations (10, 12, 14 μg/mL) for OFL, FLV, and CPD recurred three times within the day.
[c] Mean of three various concentrations (10, 12, 14 μg/mL) for OFL, FLV, and CPD recurred three times in three different days.

Table 5
Analysis laboratory prepared mixtures.

OFL (μg/mL)	FLV (μg/mL)	CPD (μg/mL)	% Recovery[a] of OFL	% Recovery[a] of FLV	% Recovery[a] of CPD
			FSD	FSD	DW
10	10	10	99.68	100.07	100.00
10	14	18	99.19	101.25	101.07
8	22	10	99.00	101.38	99.68
8	10	6	98.61	98.57	98.57
6	10	6	99.21	99.91	98.95
	Mean% ± SD		99.23 ± 0.388	100.24 ± 1.143	99.66 ± 0.976

[a] Mean of three determinations.

3.3. Greenness assessment of the developed methods

Green chemistry strategies have received interest in research [25,33–36]. The environmental friendliness profile of the analytical procedures was reported as a numerical number by the AGREE tool. The measured result, which was 0.8, supported the devised method's green properties (Fig. S6).

4. Validation

4.1. Linearity

To establish the linearity of the recommended techniques, various quantities of OFL (2–14 μg/mL), FLV (2.5–30 μg/mL), and CPD (6–30 μg/mL) were examined together. Each concentration was repeated three times. The analysis was conducted using the same experimental methodologies as those previously mentioned. **Table (4)'s** findings for linear regression equations were clear.

4.2. Range

As shown in **Table (4)**, the calibration's range was created using the practical range demanded by adherence to Beer's law and the concentration of all OFL, FLV, and CPD that were present in their combined dose form in order to deliver linear, precise, and correct results.

4.3. LOD and LOQ

The SD of the intercept and the slope of the calibrated calibration graph were used to determine the LOD and LOQ for each OFL, FLV, and CPD in accordance with ICH guidelines. For this reason, calibration graphs for each medication under study produced in a linearity examination were used. **Table (4)** presented the findings and demonstrated the sensitivity of the utilized spectrophotometric methods.

Table 6
Statistical analysis of the adopted spectroscopic methods and the reported methods for simultaneous determination of OFL, FLV, and CPD mixtures.

Parameters	OFL				FLV				CPD			
	Reported method	PLS	GA-PLS	FSD	Reported method	PLS	GA-PLS	FSD	Reported method	PLS	GA-PLS	DW
Mean	99.32	99.63	99.59	99.83	100.75	100.30	100.10	100.66	101.20	100.27	100.11	101.33
S.D.	0.970	0.569	0.566	0.594	0.890	0.604	0.751	0.503	1.250	0.807	0.997	0.417
n	3	3	3	3	3	3	3	3	3	3	3	3
Variance	0.941	0.324	0.320	0.353	0.792	0.365	0.564	0.253	1.563	0.651	0.994	0.174
t-test	(2.78)[a]	0.48	0.42	0.78	(2.45)[a]	0.85	1.10	0.17	(2.78)[a]	1.08	1.18	0.18
F- test	(19)[a]	2.91	2.94	2.66	(19)[a]	2.17	1.40	3.14	(19)[a]	2.40	1.57	9.00

[a] The data between parentheses represent the critical t and F values

Table 7
Application of standard addition technique for the analysis of the laboratory prepared combined dosage form utilizing the proposed methods.

Drug	Pharmaceutical taken (μg/mL)	Pure added (μg/mL)	Pharmaceutical found[a] (μg/mL)	Recovery[b] (%R)
				FSD
OFL	10	2	9.98	100.18
		3		99.85
		4		98.62
	Mean ± %RSD			99.55 ± 0.824
	Pharmaceutical taken (μg/mL)	**Pure added (μg/mL)**	**Pharmaceutical found [a] (μg/mL)**	**Recovery [b] (%R)**
				FSD
FLV	10	2	10.07	101.84
		3		99.69
		4		99.40
	Mean ± %RSD			100.31 ± 1.329
CPD	**Pharmaceutical taken (μg/mL)**	**Pure added (μg/mL)**	**Pharmaceutical found [a] (μg/mL)**	**Recovery [b] (%R)**
	10	2	10.13	**DW**
		3		100.79
				98.52
		4		100.36
	Mean ± %RSD			99.89 ± 1.206

[a] Mean of three determinations.
[b] Mean of three determinations.

4.4. Accuracy

The acceptable recoveries percentage (R%) achieved after determining three varied concentration levels (10, 12, 14 μg/mL) for all studied drugs across the established linearity range Table (4) supported the accuracy of the developed methodologies.

Furthermore, the accuracy was tested using standard addition technique, which included adding various known concentrations of pure standards to the dosage form. The developed spectrophotometric procedures generated adequate results, which are shown in Table (7) as well R% and relative standard deviation (RSD).

4.5. Precision

Triplicates of three distinct concentrations (10, 12, 14 μg/mL) for each OFL, FLV and CPD were analyzed by the developed spectrophotometric methods on the same day as well as three subsequent days to assess the repeatability and intermediate precision of the proposed methods. The allowable estimated RSD for each concentration was shown in Table (4).

4.6. Selectivity

The selectivity of the proposed methods was determined by analyzing several varying lab-prepared combinations of OFL, FLV and CPD within the obtained linearity range. Table (5) showed that the developed spectrophotometric approaches led to satisfactory results.

4.7. Spectrophotometric stability of standard solutions

The lack of any strange peaks, variations in peak locations, or weakening of the intensity of significant peaks served as spectrophotometric evidence of the prepared standards' stability. The standards were found to be stable at refrigeration temperature (4 °C), with intact spectra for 15 days.

5. Analysis of pharmaceutical dosage form

The developed methods were successfully implemented to the dosage form to determine the concentration of each component. The synthesized dosage form analysis results were summarized in Table (6).

6. Application in human spiked plasma

The proposed method had been applied for the determination of the studied drugs in their maintenance plasma levels. The FLV was rapidly metabolized in plasma to the main metabolite 3-methylflavone-8-carboxylic acid, so to solve this we utilized the procedure innovated by M. Bertoli et al. which utilized the sodium bicarbonate 5 % solution added to plasma immediately after sampling to deactivate the esterase enzymes that could degrade FLV to the main metabolite to guarantee accuracy of the determination [23]. Diethyl ether was chosen as the organic phase during the liquid/liquid extraction due to the compromised solubility of the three drugs into it. The recovery percentage of each component (R %) was summarized in Table (8).

Table 8
Application of proposed spectrophotometric methods in spiked human plasma utilizing the GbD based FSD-DW coupled methodology.

OFL			FLV			CPD		
Added (μg/mL)	Found[a] (μg/mL)	%Recovery	Added (μg/mL)	Found[a] (μg/mL)	%Recovery	Added (μg/mL)	Found[a] (μg/mL)	%Recovery
2.5	2.34	93.53	2.5	2.39	95.92	14	13.19	94.20
3	2.84	94.87	3	2.83	94.26	15	14.19	94.63
3.5	3.33	95.12	3.5	3.30	94.31	16	15.61	97.56
Mean ± %RSD		94.51 ± 0.905	Mean ± %RSD		94.83 ± 0.993	Mean ± %RSD		95.46 ± 1.913

[a] Average of three determinations.

Table 9
One-way ANOVA statistical analysis within 95 % confidence interval on the recovery percentage data obtained from application of the spectroscopic methods and the reported spectrophotometric methods on the laboratory prepared combined dosage form.

Drugs	Source	Degree of Freedom	Sum of squares	Mean square	F-value	p-value
OFL	Between Groups	3	0.392	0.131	0.793	0.531
	Within Groups	8	1.319	0.165		
FLV	Between Groups	3	0.486	0.162	0.309	0.819
	Within Groups	8	4.197	0.525		
CPD	Between Groups	3	3.707	1.236	1.772	0.230
	Within Groups	8	5.578	0.697		

7. Statistical analysis of the developed methods

The Student's t- and F-tests at P = 0.05 were used for the statistical assessment of the results acquired by the recommended procedures and the published methods for each medication. As can be seen in Table (6), there was no discernible change in accuracy or precision.

A one-way ANOVA was also used to assess the differences between the created approaches. Table (9) showed that there were no significant discrepancies across the methodologies, proving that the proposed Spectroscopic methods were reliable for measuring OFL, FLV, and CPD quantitatively in their combined dose form.

8. Conclusion

The final morphology of the spectrum of a compound in each solvent was determined by the intricate interplay of various factors, as explained. These factors include the molecular spin multiplicity, the electronic transitions' gap energy (ΔE) and the solute-solvent interactions (HB). The resulting spectrum reflected the subtle balance of these factors, which can be regarded as a hidden dance in the quantum realm. In addition to quantum chemical interpretations of the impact of various diluting solvents on the spectral resolution of the overlapped spectra and its reflection on the exerted analytical resolving efforts, the current study sought to provide novel rational spectroscopic solutions to resolve severely overlapping pharmaceutical mixtures. Instead of using PLS-based models to demonstrate their superior accuracy, the proposed chemometric technique based on embedding the GA algorithm in the established predictive PLS models demonstrated improved predictive profiling based on the lower validation sets values in GA-PLS models. Additionally, as compared to the chemometric and the published techniques, the developed univariate spectroscopic methodologies augmented by GbD showed improved resolving capabilities toward the examined ternary combination and no discernible statistical difference. Moreover, the ecological impact of the current study was considered and fulfilled in all aspects of the conducted experiments as proved from the outstanding score obtained from the applied AGREE assessment protocol.

Data availability

Data will be made available on request.

CRediT authorship contribution statement

Maya S. Eissa: Visualization, Validation, Supervision. **Khaled Attala:** Writing – original draft, Formal analysis, Data curation. **Ahmed Elsonbaty:** Writing – review & editing, Writing – original draft, Validation, Formal analysis, Data curation, Conceptualization. **Aziza E. Mostafa:** Writing – review & editing, Supervision. **Randa A. Abdel Salam:** Writing – review & editing, Supervision, Project administration. **Ghada M. Hadad:** Writing – review & editing, Supervision, Project administration. **Mohamed A. Abdelshakour:** Writing – review & editing, Supervision, Methodology.

Declaration of competing interest

The authors declare that they have no known competing financial interests or personal relationships that could have appeared to influence the work reported in this paper.

Appendix A. Supplementary data

Supplementary data to this article can be found online at https://doi.org/10.1016/j.heliyon.2024.e24466.

References

[1] H.O. Hammod, UTI in primary care : are we prescribing too much, SAS J. Med. 9 (2023) 860–864, https://doi.org/10.36347/sasjm.2023.v09i08.011.
[2] P.A. Todd, D. Faulds, Ofloxacin: a reappraisal of its antimicrobial activity, pharmacology and therapeutic use, Drugs 42 (1991) 825–876, https://doi.org/10.2165/00003495-199142050-00008.
[3] R. Finch, P. Davey, M. Wilcox, W. Irving, Inhibitors of bacterial cell wall synthesis, Antimicrob, Chemother 11–24 (2014), https://doi.org/10.1093/med/9780199697656.003.0010.
[4] S.S. Agrawal, S.B. Bhagat, K. Krishnaprasad, Retrospective cohort study analyzing clinical utility of cefpodoxime-ofloxacin combination in patients with community-acquired infection at different outpatient setting across India, Int. J. Sci. Study. 5 (2017) 180–183, https://doi.org/10.17354/ijss/2017/185.
[5] D.C. Angst, B. Tepekule, L. Sun, B. Bogos, S. Bonhoeffer, Comparing treatment strategies to reduce antibiotic resistance in an in vitro epidemiological setting, Proc. Natl. Acad. Sci. U. S. A. 118 (2021) 1–7, https://doi.org/10.1073/PNAS.2023467118.
[6] K. Hesch, Agents for treatment of overactive bladder: a therapeutic class review, Baylor Univ. Med. Cent. Proc. 20 (2007) 307–314, https://doi.org/10.1080/08998280.2007.11928310.
[7] P. Cazzulani, R. Panzarasa, C. Luca, D. Oliva, G. Graziani, Pharmacological studies on the mode of action of flavoxate, Arch. Int. Pharmacodyn. Ther. 268 (1984) 301–312.
[8] E.S. Rovner, A.J. Wein, Antimuscarinic drugs for the treatment of female urinary incontinence, Women's Heal. 2 (2006) 251–265, https://doi.org/10.2217/17455057.2.2.251.
[9] S.V. Gandhi, U.P. Patil, N.G. Patil, Simultaneous spectrophotometric determination of cefpodoxime proxetil and ofloxacin in tablets, Hindustan Antibiot. Bull. 51 (2009) 24–28.
[10] M. Attimarad, Simultaneous determination of ofloxacin and flavoxate hydrochloride by absorption ratio and second derivative UV spectrophotometry, J. Basic Clin. Pharm. 2 (2010) 53–61.
[11] S.S. Ainwale, V.D. Chipade, A.P. Dewani, R.L. Bakal, M.R. Shiradkar, A. V Chandewar, Simultaneous rp-Hplc determination of cefpodoxime proxetil and ofloxacin, Int. Res. J. Pharm. 6 (2015) 677–681, https://doi.org/10.7897/2230-8407.069132.
[12] M. Attimarad, Simultaneous determination of ofloxacin and flavoxate hydrochloride by absorption ratio and and second derivative UV spectrophotometry, J. Basic Clin. Pharm. 2 (2011) 53–61.
[13] A. Elsonbaty, M.S. Eissa, W.S. Hassan, S. Abdulwahab, Separation-free spectrophotometric platforms for rapid assessment of combined antiplatelet therapy in complex matrices, Bioanalysis 12 (2020) 335–348, https://doi.org/10.4155/bio-2019-0293.
[14] A. Elsonbaty, A. Serag, S. Abdulwahab, W.S. Hassan, M.S. Eissa, Analysis of quinary therapy targeting multiple cardiovascular diseases using UV spectrophotometry and chemometric tools, Spectrochim. Acta Part A Mol. Biomol. Spectrosc. 238 (2020) 118415, https://doi.org/10.1016/j.saa.2020.118415.
[15] A. Elsonbaty, K. Attala, An eco-friendly modified methodology for the resolution of binary pharmaceutical mixtures based on self-deconvolution of the UV spectrophotometric spectra in the Fourier domain: application of Fourier self-deconvolution in UV spectroscopy, Spectrochim. Acta Part A Mol. Biomol. Spectrosc. 264 (2022) 120262, https://doi.org/10.1016/j.saa.2021.120262.
[16] A. Elsonbaty, A.W. Madkour, A.M. Abdel-Raoof, A.H. Abdel-Monem, A.-A.M.M. El-Attar, Computational design for eco-friendly visible spectrophotometric platform used for the assay of the antiviral agent in pharmaceutical dosage form, Spectrochim. Acta Part A Mol. Biomol. Spectrosc. 271 (2022) 120897, https://doi.org/10.1016/j.saa.2022.120897.
[17] M.S. Eissa, A. Elsonbaty, K. Attala, R.A. Abdel Salam, G.M. Hadad, M.A. Abdelshakour, A.E. Mostafa, Innovative and sustainable deconvoluted amplitude factor spectrophotometric method for the resolution of various severely overlapping pharmaceutical mixtures: applying the complex-GAPI-tool, Heliyon 9 (2023) e20152, https://doi.org/10.1016/j.heliyon.2023.e20152.
[18] T. Hanai, Molecular modeling for quantitative analysis of molecular interactions, in: Lett. Drug Des. Discov., Bentham Science Publishers, 2005, pp. 232–238, https://doi.org/10.2174/1570180053765192.
[19] M.A. Abdelshakour, M.S. Eissa, K. Attala, A. Elsonbaty, R.A. Abdel Salam, G.M. Hadad, A.E. Mostafa, Greenness-by-design approach for developing novel UV spectrophotometric methodologies resolving a quaternary overlapping mixture, Arch. Pharm. (Weinheim) (2023) e2300216, https://doi.org/10.1002/ardp.202300216.
[20] S. Gould, Urinary tract disorders. Clinical comparison of flavoxate and phenazopyridine, Urology 5 (1975) 612–615, https://doi.org/10.1016/0090-4295(75)90111-9.
[21] F. Bressolle, F. Gonçalves, A. Gouby, M. Galtier, Ofloxacin clinical pharmacokinetics, Clin. Pharmacokinet. 27 (1994) 418–446, https://doi.org/10.2165/00003088-199427060-00003.
[22] V. Kumar, R. Madabushi, M.B.B. Lucchesi, H. Derendorf, Pharmacokinetics of cefpodoxime in plasma and subcutaneous fluid following oral administration of cefpodoxime proxetil in male beagle dogs, J. Vet. Pharmacol. Ther. 34 (2011) 130–135, https://doi.org/10.1111/j.1365-2885.2010.01198.x.
[23] M. Bertoli, F. Conti, M. Conti, A. Cova, I. Setnikar, Pharmacokinetics of flavoxate in man, Pharmacol. Res. Commun. 8 (1976) 417–428, https://doi.org/10.1016/0031-6989(76)90041-2.
[24] S. Alex, H. Le Thanh, D. Vocelle, Studies of the effect of hydrogen bonding on the absorption and fluorescence spectra of all-trans-retinal at room temperature, Can. J. Chem. 70 (1992) 880–887, https://doi.org/10.1139/v92-117.
[25] A.E. Mostafa, A. Elsonbaty, K. Attala, M.A. Abdelshakour, R.A. Abdel Salam, G.M. Hadad, M.S. Eissa, Miniaturized chip integrated ecological sensor for the quantitation of milnacipran hydrochloride in the presence of its impurities in dosage form and human plasma, J. Electrochem. Soc. 170 (2023) 087504, https://doi.org/10.1149/1945-7111/ace9fd.
[26] A. Belay, E. Libnedengel, H.K. Kim, Y.H. Hwang, Effects of solvent polarity on the absorption and fluorescence spectra of chlorogenic acid and caffeic acid compounds: determination of the dipole moments, Luminescence 31 (2016) 118–126, https://doi.org/10.1002/bio.2932.
[27] H. McConnell, Effect of polar solvents on the absorption frequency of n→ electronic transitions, J. Chem. Phys. 20 (1952) 700–704, https://doi.org/10.1063/1.1700519.
[28] A. Albini, S. Monti, Photophysics and photochemistry of fluoroquinolones, Chem. Soc. Rev. 32 (2003) 238–250, https://doi.org/10.1039/b209220b.
[29] J. Catalán, J.P. Catalán, On the solvatochromism of the n ↔ π* electronic transitions in ketones, Phys. Chem. Chem. Phys. 13 (2011) 4072–4082, https://doi.org/10.1039/c0cp02282a.
[30] A.I. Adeogun, N.W. Odozi, N.O. Obiegbedi, O.S. Bello, Solvents effect on n→π* and π→π* transition of 9-fluorenone, African J. Biotechnol. 7 (2008) 2736–2738.

[31] A. Köhler, J. Wilson, Phosphorescence and spin-dependent exciton formation in conjugated polymers, Org. Electron. 4 (2003) 179–189, https://doi.org/10.1016/j.orgel.2003.08.011.
[32] D.M. Haaland, E. V Thomas, Partial least-squares methods for spectral analyses. 1. Relation to other quantitative calibration methods and the extraction of qualitative information, Anal. Chem. 60 (1988) 1193–1202.
[33] A.E. Mostafa, M.S. Eissa, A. Elsonbaty, K. Attala, R.A. Abdel Salam, G.M. Hadad, M.A. Abdelshakour, Computer-Aided design of eco-friendly imprinted polymer decorated sensors augmented by self-validated ensemble modeling designs for the quantitation of drotaverine hydrochloride in dosage form and human plasma, J. AOAC Int. (2023), https://doi.org/10.1093/jaoacint/qsad049 qsad049.
[34] M.A. Abdelshakour, K. Attala, A. Elsonbaty, R.A. Abdel Salam, G.M. Hadad, A.E. Mostafa, M.S. Eissa, Eco-friendly UV-spectrophotometric methods employing magnetic nano-composite polymer for the extraction and analysis of sexual boosters in adulterated food products: application of computer-aided design, J. AOAC Int. (2023) qsad084.
[35] K.D. Otaif, M.M. Fouad, N.S. Rashed, N.Y.Z. Hosni, A. Elsonbaty, E. Elgazzar, Green Prospective Approach of Chromium Zinc Oxide Nanoparticles for Highly Ultrasensitive Electrochemical Detection of Anti-hypotensive Medication in Various Matrices, ACS Omega 8 (2023) 30081–30094. https://doi.org/10.1021/acsomega.3c02381.
[36] A. Elsonbaty, W.S. Hassan, M.S. Eissa, S. Abdulwahab, Micelle-incorporated liquid chromatography in the light of green chemistry: an application for the quality control analysis of anti-platelet fixed-dose combinations, J. AOAC Int. 105 (2022) 1228–1233, https://doi.org/10.1093/jaoacint/qsac046.